Canadian Science Publishing
NRC Research Press journals | Publishing Services

Canadian Geotechnical Journal
Revue canadienne de géotechnique

FIELD HYDROLOGICAL MONITORING OF A SLOPING SHALLOW PYROCLASTIC DEPOSIT

Journal:	*Canadian Geotechnical Journal*
Manuscript ID	cgj-2015-0344.R2
Manuscript Type:	Article
Date Submitted by the Author:	14-Jan-2016
Complete List of Authors:	Comegna, Luca; Seconda Università degli Studi di Napoli, Department of Civil Engineering, Design, Building and Environment Damiano, Emilia; SecondaUniversità di Napoli, Ingegneria Civile Greco, Roberto; SecondaUniversità di Napoli, Ingegneria Civile Guida, Andrea; Seconda Università degli Studi di Napoli, Department of Civil Engineering, Design, Building and Environment; Olivares, Lucio; Department of civil Engineering - SECOND UNIVERSITY OF NAPLES Picarelli, Luciano; Seconda Università di Napoli, Dpt of Civil Engineering
Keyword:	hydrological slope response, automatic monitoring, unsaturated granular soils

FIELD HYDROLOGICAL MONITORING OF A SLOPING SHALLOW PYROCLASTIC DEPOSIT

Luca Comegna[(1)]*, Emilia Damiano[(1)], Roberto Greco[(1)], Andrea Guida[(1)], Lucio Olivares[(1)] and Luciano Picarelli[(1)]

(1) Seconda Università degli Studi di Napoli

Department of Civil Engineering, Design, Building and Environment

via Roma 29, 81031 Aversa (CE), Italy

* Corresponding author

Luca Comegna

e-mail: luca.comegna@unina2.it

phone: 0039-081-5010384, fax: 0039-081-5037370

Abstract

Many mountainous areas in Campania, Southern Italy, are characterised by steep slopes covered by unsaturated volcanic deposits. Shallow landslides are frequently triggered by intense and persistent rainfall events, often turning into debris flows, that cause huge damage and casualties. Field hydrological monitoring is an useful tool to develop consistent models of slope response to rainfall, in terms of soil suction and moisture, and to define landslide triggering conditions. This was one of the reasons why since 2002 field monitoring is being carried out in Cervinara, around 50 km North-East of Naples. Since October 2009, rainfall height, soil suction and water content at several locations and depths along the slope are automatically being monitored. The data collected help to demonstrate the effectiveness of such a system for better understanding the hydrological processes occurring in similar slopes of Campania, allowing to distinguish between seasonal suction fluctuations, related to long-term meteorological forcing, and short-term response to rainstorms.

Key-words: hydrological slope response, automatic monitoring, unsaturated granular soils.

1 Introduction

The stability of slopes covered by unsaturated deposits is frequently assured by matric soil suction, which significantly contributes to the soil shear strength (Fredlund and Rahardjo 1993). In fact, capillary forces provide an additional strength component, usually known as apparent cohesion, that allows the slope to remain stable at angles much larger than the soil internal friction angle. This aspect is particularly pregnant in slopes featured by rather shallow covering deposits, where also a small value of apparent cohesive intercept is able to grant a not negligible contribution to the safety factor.

The alternating seasonal climate conditions are responsible of a continuous fluctuation in the landslide hazard, whose reliable assessment is strictly affected by the knowledge of the slope response to weather factors (Cascini et al. 2014). In fact, while during warm seasons the soil usually experiences high matric suction due to evapotranspiration processes, during wet seasons rain-water infiltration is responsible of an increase in moisture content that causes matric suction decrease. Precipitation, if particularly intense and prolonged, could also induce the development of positive pore-water pressure within the piroclastic cover (because of a downward decreasing hydraulic conductivity) or at the soil-bedrock interface (if the bedrock is featured by a permeability lower than that of the soil cover).

Field monitoring is an useful tool to develop reliable models of slope hydrological response. Thanks to the increased availability of high quality and low cost sensors and data-loggers, a number of researchers is recently working on this subject, providing interesting data at high temporal resolution. Such studies are primarily aimed to explain the failure mechanism of different occurred shallow landslides in unsaturated soils in relation to rainfall patterns. For instance, Tsaparas et al. (2003) show the results of a 1-year long field monitoring, consisting in the automatic acquisition of matric suction and positive pore-water pressure, until a depth of 3.2 m below the ground surface, induced by natural and simulated rainfall events on two embankments in residual soils in

Singapore. Li et al. (2005) present the results of a full-scale field experiment conducted to reveal the surface infiltration process within a saprolite slope in Hong Kong, instrumented with soil moisture probes, tensiometers and piezometers. Zhan et al. (2007) use tensiometers, moisture probes and a flow metre to study the infiltration characteristics and runoff amounts of a naturally grassed cut slope in China. Trandafir et al. (2008) report the suction changes, induced by different rainstorm events, monitored within a 1.2 thick deposit in residual soils covering a natural slope in Japan. Hawke and McConchie (2011) monitor the fluctuating soil volumetric water content and the piezometric regime up to the depth of 1 m induced by rainfall events over a 5-year period on a natural slope in New Zealand. Again in New Zealand, Harris et al. (2012) develop a specific early warning system for a roadway embankment, based on the measured variation of the volumetric water contents induced by rainfall. Chae and Seo (2012) describe a monitoring system realized to observe soil moisture changes until the depth of 80 cm during rainfall events involving a natural valley in Korea. Collins et al. (2012) show both the soil moisture and the piezometric regime (up to the depth of 1.4 m) observed during a 1-year long monitoring of a natural slope in California, USA. Smith et al. (2014) illustrate the measurements of rainfall, volumetric water content, matric suction and positive pore-water pressures, registered up to a depth lower than 3 m, coming from a 3-year long automatic monitoring system installed in a headwater basin in Oregon, USA.

The results of the previously cited monitoring sites highlight, in particular, that pressure variation induced by rainstorms is controlled by the rainfall features (duration and intensity) as well as by the initial soil-moisture conditions.

Since 2002, the research team of the Seconda Università di Napoli has been monitoring a shallow deposit in unsaturated pyroclastic soils covering a steep slope located in Cervinara, Southern Italy, where in 1999 a rainfall-induced flowslide occurred. Recently, the installed devices have been integrated for automatic reading of matric suction and volumetric water content at different depths (Comegna et al. 2011; Guida et al. 2012). Since then, the amount of collected information has enormously increased, allowing detailed investigations of moisture movements

within the pyroclastic cover under individual storms, leading to the development of mathematical models of the hydrological response of the cover to precipitations (Comegna et al. 2013; Greco et al. 2013). The main goal of this paper is to understand the relationship between rainfall events and the short-term response of the monitored deposit, giving particular attention to the role played by the initial soil conditions, in turn related to the hydrological response to long-term meteorological forcing.

2 Monitored site

2.1 Geomorphological and geotechnical framework

In order to capture the main effects of precipitations on the stability conditions of slopes in unsaturated pyroclastic soils, widespread in a vast area around Naples, in 2002 a pilot study was initiated by monitoring the Mount Cornito hillslope, at a couple of kilometres upslope the town of Cervinara, about 50 km northeast of Naples, that was involved in a catastrophic flowslide on December 16th, 1999 (Figure 1), that caused five victims. The landslide was triggered by a rainstorm of 320 mm in 50 hours, with a maximum hourly intensity, I_{max} = 19 mm/h (Olivares and Picarelli 2003).

Regarding the geomorphological features of the monitored site, a thorough description is provided by literature (Fiorillo et al. 2001; Olivares and Picarelli 2003; Picarelli et al. 2006; Damiano et al. 2012). The town of Cervinara is located at the base of the northern side of the Partenio Mountains, along the southern edge of the Caudina valley. The basal formation, constituted by Mesozoic–Cenozoic fractured limestones, is covered by airfall pyroclastic deposits, as ashes and pumices, that are the result of the volcanic activity of Somma–Vesuvius and Phleagraean Fields, alternated with buried soils. In the Campania hilly regions that are mainly mantled by airfall deposits, the covering soils are layered at an angle very close to the bedrock surface, and their thickness tends to strongly decrease with such inclination, ranging from some

decimetres in the steepest upslope zones (50°-90° inclined) to more than ten metres at the foot of the hill (Guadagno et al. 2011). Particularly regarding the studied slope, facing North-East at about 560 m above sea level (a.s.l.) and adjoining the 1999 flowslide (Figure 1), the maximum depth of the covering deposit is typically less than 2.5 m along the 40° inclined upslope zone; on the contrary, it reaches tens of metres at the foot of the slope, where the cover consists of a mixture of pumices and remoulded ashes, as a result of colluvium accumulation.

The studied slope is covered by regularly cultivated chestnut trees. Based on geological surveys and geotechnical investigations (Olivares and Picarelli 2003), the pyroclastic soil mantle cover recognized under the topsoil, which is constituted by humified volcanic ash, includes the following layers: A) coarse pumices, attaining a maximum thickness of 40 cm; B) volcanic ashes, with thickness ranging between 1.0 m and 1.7 m; C) fine pumices, 0.3-0.6 m thick; D) altered ashes, 0.1-0.8 m thick, directly covering the fractured calcareous bedrock. Some of these layers are locally missing, possibly as a result of past landslides or erosive processes. The occurred landslide involved all layers except the deepest one (layer D).

An accurate geotechnical characterization of the soils is provided by Damiano et al. (2012), who report the results of different laboratory tests performed on a number of undisturbed and remoulded soil samples. Figure 2 shows the grain-size of the various layers, spanning sandy gravels (layer A) and sandy silts (layer D). The finest component of ashes (layers B and D) is featured by a plasticity index ranging in the interval 10-30 %. All layers are unsaturated, and their degree of saturation is strongly governed by weather conditions. Their unit weight ranges in the interval 13-16 kN/m^3. The overall porosity of volcanic ashes (layer B), about 70%, is higher than the one of altered ashes (layer D), featured by a value of about 60%, and also than the porosity of pumices (layers A and C), lower than 60%.

Laboratory tests were carried out in oedometer and triaxial tests in order to obtain information about saturated hydraulic conductivity. As shown by the results reported in Table 1, referred to the range of mean effective stress 20-150 kPa, the lowest and highest values were respectively

measured for layer C (k_{sat} = 3E-07 m/s) and layer A (k_{sat} =7E-06 m/s). Data about the unsaturated hydraulic conductivity were also available for layer B: the experimental data showed that the minimum permeability, corresponding to the maximum likely suction typically measured in situ (about 80 kPa), is equal to 1E-08 m/s.

Drained and undrained triaxial tests were also performed on natural specimens in order to know the saturated strength parameters of ash B and D. According to the corresponding results, the ash B is featured, at effective mean stress in the interval 20-150 kPa, by a nil cohesion and a friction angle φ′ = 38°, while the altered ash D has a cohesion c' = 11 kPa and a friction angle φ′ = 31°. Moreover, Olivares and Picarelli (2003) investigated the role of suction on the shear strength of ash B through a series of drained suction controlled triaxial tests. The Authors, after elaborating the experimental data by extending the Mohr–Coulomb criteria for unsaturated soil and assuming the measured saturated friction angle φ′ = 38°, found that the apparent cohesive intercept increases from 1.5 kPa to 10 kPa for suction ranging in the interval 2-80 kPa. In particular, they estimate such relation

$$c_{(u_a-u_w)}[kPa] = 2.38 \cdot \ln(u_a - u_w) - 0.17 \qquad [1]$$

as interpolating function linking the apparent cohesive intercept, $c_{(u_a-u_w)}$, to the matric suction, u_a-u_w.

2.2 Description of the monitoring station

Monitoring at the slope started in 2002 by measurements of both rainfall height and soil suction (Olivares et al. 2003; Damiano et al. 2012). Hourly precipitations were measured by a rain gauge having a sensitivity of 0.2 mm. Soil suction was measured by twelve "*Jet-fill*" tensiometers, installed at five locations along the slope, at various depths between 0.60 and 2.40 m (Figure 1). The tensiometers were equipped with a Bourdon manometer and the readings were manually taken about every two weeks: as a consequence, it was possible to collect discontinuous information

about only the long-term hydrological slope response. Therefore, in order to have continuous data, necessary to deeply investigate the short term slope response to precipitations, an additional automatic monitoring station has been installed in 2009 (Figure 1). It consists of two nests of suction and moisture sensors, located 5 m far from each other (Figure 3). All transducers are connected to a Campbell Scientific Inc. CR-1000 Data Logger for the automatic data acquisition and storage, with a time resolution of two hours. The entire monitoring station is powered by a solar panel with a 12V backup battery.

The local stratigraphy, recognized by pits dug near nest 1 up to a depth z = 1.90 m (Figure 3a), consists of three layers: i) top soil, 10 cm thick; ii) volcanic ash (layer B), 170 cm thick; iii) altered ash (layer D), 10 cm thick. The stratigraphy close to nest 2 (Figure 3b) differs from the previous one because of the presence of a 40 cm thick coarse pumices layer (layer A) located between the top soil and the volcanic ash. Therefore, at both the locations, the fine pumices (layer C, which had been found elsewhere along the same slope) were not found.

Suction is measured by eight "*Jet-fill*" tensiometers equipped with a tension transducer. Four of them were installed in August, 2009, at nest 1, at depths between 0.60 and 1.70 m (Figure 2a). The last four tensiometers were installed in October, 2010, at nest 2, at depths from 0.60 m to 1.70 m, (Figure 2b). The ceramic tips of all the tensiometers were located in the ashy layers. Concerning installation, the probe was pushed into the soil by crossing a small hole, previously dug by a small drill. A rigid cylinder was inserted to sustain the hole during excavation crossing the pumice layers: the excavated soil was thus used to fill the gap around the tensiometer tube. Moreover, in order to avoid any water infiltration alongside the tube, the part of the hole located next to the ground surface was filled with a bentonite–cement mixture. A careful maintenance was granted by regularly checking the complete saturation of the instruments, (that was assured by adding within the tube de-aired water necessary to remove possible air bubbles), especially after long-lasting dry periods and by controlling the instruments after winter days featured by particularly low air temperatures that could freeze the contained water.

Soil volumetric water contents are measured by seven probes for Time Domain Reflectometry (TDR), which are connected through coaxial cables and a multiplexer to a Campbell Scientific Inc. TDR-100 reflectometer. The probes have three metallic rods of the diameter of 3 mm, spaced 15 mm apart from each other. The probe lengths are between 100 mm and 400 mm. TDR readings provide the value of the soil bulk dielectric permittivity, ε_r, which can be related to the soil volumetric water content, θ, through a calibration relationship, as explained by Topp et al. (1980). For the soils at the study site, a specific relationship has been established in laboratory experiments by Guida et al. (2012) on undisturbed ash samples and reconstituted pumices taken nearby the monitoring station, allowing to obtain an average error in the estimated volumetric water content of $\pm 0.02 m^3/m^3$ (Topp et al., 1980). Four TDR probes were buried at various depths at nest 1 in August, 2009 (Figure 3a). Three more probes were installed at nest 2 in October 2010 (Figure 3b). All the sensors were placed vertically in the soil. Some of them were located very close to the ceramic tips of the tensiometers, in order to allow coupling water content and suction at the same location.

A general framework of the long-term hydrological slope response and examples of the short-term effects of individual rainstorms are presented in the following, with special reference to the role played by rainfall features and by soil properties.

3 Discussion of monitoring data

3.1 Long-term hydrological response

As already pointed out, rainfall data have been measured by a rain gauge installed at the experimental field since 2002. Such data are consistent with those provided by the nearby rain gauge of San Martino Valle Caudina, managed by the Regional Civil Protection Agency and located about 4 km from the slope, at an elevation similar to that of monitoring site. In particular, data recorded since 1965 show that the mean annual rainfall is about 1300 mm, with average monthly values ranging from 30 mm in July to 190 mm in November. Air temperature data is not

available at the San Martino Valle Caudina station, but has been provided since 2001 by the Pietrastornina station (located at 495 m a.s.l. and 15 km from Cervinara). The mean lowest daily air temperature, 3°C, and the mean highest daily temperature, 30°C, are respectively attained in February and in August, as typical of Northern hemisphere temperate regions.

Figure 4 and Figure 5 show hourly values of suction and volumetric water content, the hourly hyetograph and the daily mean temperature, from December, 2009, to December, 2011. Minimum and maximum monthly values of suction are reported in Table 2 and Table 3. As expected, the lowest value is attained at every depth during the wet season, while the highest one is reached during the warm season. Similar trends have been observed also in other pyroclastic slopes of Campania Region (Cascini and Sorbino 2004; Evangelista et al. 2008; Pirone et al. 2010; Cascini et al. 2014).

Concerning the data of 2011 (Figure 5), the lowest suction, comprised between 1.8 kPa and 4.2 kPa depending on the depth, was attained between January and March, a period characterized by frequent rainstorms (40% of the total cumulative rainfall of 2011) and by a mean daily temperature ranging between 8°C and 11°C (Figure 5). According to Equation [1], suggested by Olivares and Picarelli (2003), the apparent cohesive strength, $c_{(u_a - u_w)}$, related to such suction values should oscillate in the range 1.2-3.3 kPa. The corresponding additional strength could significantly influence the factor of safety, *FS*, of slopes covered by shallow deposits. For instance, taking into account the simplified infinite model, suitable to evaluate the stability conditions of the analyzed Cervinara case, and assuming a homogeneous deposit featured by slope angle $\alpha = 40°$, unit weight $\gamma = 14$ kN/m^3, $c' = 0$ and $\varphi' = 38°$, the corresponding *FS* at a considered depth, *z*, could be estimated by the following formulation

$$FS = \frac{tg\varphi'}{tg\alpha} + \frac{c_{(u_a - u_w)}}{\gamma \cdot z \cdot sen\alpha \cdot \cos\alpha} \qquad [2]$$

thus providing $FS = 1.1$ as minimum value, that coincides with the lowest annual value. During the same time interval, the monthly mean suction ranged between 5 kPa, at the greatest depth, and 10.5 kPa, at the shallowest depth (Figure 6b).

In April and May, when the monthly precipitation was in both months 96 mm (only one third of the rainfall fallen during March) and the mean air temperature between 15°C and 18°C, an increasing trend of suction of about +0.1 kPa per day was measured at every depth, leading to a suction of 17 kPa at 0.60 m at the end of the period.

In June, the monthly rainfall was 37 mm, while the mean temperature grew to 23°C. As a consequence, at every depth the daily suction increase was about +0.3 kPa per day, attaining at the end of the month a suction of 29 kPa close to the ground surface.

During summer, the mean temperature increased still more, reaching nearly 25°C, and a stronger daily suction growth was observed, reaching about +0.4 kPa/day at the shallowest sensors, and +0.8 kPa/day at the deepest ones. The peak value of suction, about 70 kPa, was measured in August by the deepest tensiometers. It's worth noting that such peak is probably limited by the maximum measurement range allowed by tensiometers (Fusco et al. 2013; Napolitano et al. 2015), thus it could be also higher during warmest periods. Nevertheless, thanks to the corresponding apparent cohesive values, ranging during August in the interval 9-10 kPa, the safety factor (corresponding to the highest annual value) estimated through Equation [2] should be at least equal to 1.8.

In 2011, the dry season, characterised by a few isolated rainfall events, substantially continued until November, thus soil suction remained higher than usual, especially at the highest investigated depths. However, frequent precipitations in December caused a fast reduction of suction, which soon dropped to the typical values of the wet season.

As already observed, the reduction in suction of the shallowest soil layers in response to rainfall is rapid and significantly higher than at greater depth. Therefore, the lowest values of suction are generally measured close to the ground surface. This mostly depends on the delayed and decreasing effects of infiltration with depth. However, an additional role is played by pumice layers that cut the

downward flow especially when they are far from saturation (Olivares and Tommasi 2008; Mancarella et al. 2012). Indeed, as indicated by the measurements of the TDR probe S2-3, at 0.3 m below the ground surface (nest 2), the water content of pumices rarely approaches 0.30 (Figure 5). At such a low water content, caused by their scarce water retention at high values of suction, the hydraulic conductivity is so low to hinder the downward wetting process. Such a consideration is confirmed by comparing the readings of the sensor located at 1.0 m depth in the ash at nest 2 with the values measured at the same depth at nest 1, where coarse pumices are absent. As a matter of fact, Figure 7 shows that the reduction in suction after rainfall measured in volcanic ashes by sensor L1-2 (nest 1), is higher than that measured at the same depth by sensor L2-2 (nest 2).

Figure 8 reports the calculated vertical hydraulic gradient, $i = \frac{\Delta h}{\Delta z}$, at different depths during 2011. In such an expression Δh is the difference in total head between two adjacent sensors, while Δz is the difference in elevation of their tips. It's worth noting that the monitored hydraulic gradient has never become negative, showing that, at the investigated depths, the water flux is never driven upward by evapotranspiration. However, different responses can be recognized depending on the season. In general, during wet periods the hydraulic gradient is lower than 1 at all depths, indicating that water flow is directed towards the basal surface but it is hindered by capillarity . An example of the soil suction profile observed during such period is given in Figure 8c. Only during and after intense rainfall events, the hydraulic gradient attains values higher than 1, especially next to the ground surface, due to the combined capillarity and gravity gradients. Figure 8d shows the soil suction profile in such conditions. Starting from the beginning of June, a different behaviour can be recognized at all depths. In fact, at the shallowest depths, the hydraulic gradient is initially nearly 1, thus the flow is essentially gravity driven. After the middle of July, the gradient in the shallowest investigated part of the profile starts decreasing, suggesting that an evapotranspiration flux, directed towards the ground surface, establishes across the upper soil layer; conversely, during the same period, the hydraulic gradient at higher depths constantly grows, and the flow, downward directed, tends to become mainly governed by capillarity. Such a behaviour reveals that, even when

the soil suction is well above the field capacity, the flow is still directed towards the underlying fractured bedrock. A possible interpretation of this, which anyway should be confirmed by further investigations, is that the fractures in the top few meters of the bedrock may be filled with finer material coming from the overlying soil cover (soil pockets), thus allowing, to some extent, the transmission of suction by capillarity and a redistribution of capillary water. Also, it is widely reported that weathered bedrock can significantly contribute to the availability of water for forest trees (Hubbert et al. 2001; Querejeta et al. 2006), especially during the dry season (McCole and Stern 2007; Querejeta et al. 2007), owing to the deep roots penetrating the bedrock fracture system (Witty et al. 2003; Nie et al. 2012; 2014), so that when the overlying soil is dry, water is mostly extracted from the bedrock (McCole and Stern, 2007; Nie et al. 2012). This process too might explain the downward hydraulic gradient observed during summer. A simplified mathematical model of such a hydraulic behaviour of the soil-bedrock interface was recently developed, allowing a good agreement with monitoring data (Greco et al. 2013; Greco et al. 2014). An example of the soil suction profile when the deposit is contemporarily drained from both the top and the bottom boundaries is given in Figure 8e.

By coupling matric suction and volumetric water content values measured at the same depth, local Water Retention Curves (WRCs) have been obtained (Figure 9). The scattering of the data plotted in Figure 9 is affected by measurement errors, mainly caused by the imperfect coupling of water content and suction measurements, as the two sensors, although close to each other, do not actually sample exactly the same volume of soil. However, the observed scattering is likely also due to the hysteretic behaviour already observed in the pyroclastic soils of Campania (e.g. Pirone et al. 2014; Comegna et al. 2016a; Comegna et al. 2016b), which can lead to different values of the volumetric water content for the same suction value, depending on the starting point and on the wetting or drying path. Therefore, most of such field points likely belong to different *scanning curves*, that, as known, are located between the two main curves, the *main drying curve* and the *main wetting curve*: a research, which will be also based on a specific laboratory testing

programme, is starting in order to examine in depth such aspect. The differences among the WRCs could be related to local differences in grain size (Figure 2), or in relative density. Field experimental points may be fitted by the van Genuchten (1980) equation: Figure 9 shows two curves corresponding to the upper and lower envelope of the experimental points (curve 1 and curve 3), as well as a median curve (curve 2). It's worth noting that the water content at saturation θ_s = 0.75, measured in laboratory tests on volcanic ash from layer B (Olivares et al. 2009), is much higher than the maximum one observed in situ, indicating that, since 2009, the soil never approached saturation at all the investigated depths. Moreover, the high WRC slope for suction less than 1 kPa indicates that, even starting from unusually low suction values, i.e. after a long wet season and/or intense rainstorms, full saturation requires a further great amount of water, that can be available only after extremely intense and long lasting rainstorms. It's worth pointing out that in such crucial limited interval of suction (0-1 kPa), which includes the likely lowest suction limit allowed by slope stability conditions, the TDR probes remain the only instruments able to detect the ongoing hydraulic response.

3.2 Short-term response to individual rainstorms

The high temporal resolution of monitoring allows to deeply analyze the hydrological effects of individual rainstorms. To this aim, first, a rain storm has been conventionally defined as the precipitation event during which rain never stops for more than one hour. According to such a definition, 1056 events have been identified from 2002 to 2011 with duration, D, ranging from 1 hour to 75 hours and average intensity, I_{av}, generally lower than 10 mm/h (with the exception of eight short summer storms with I_{av} comprised between 11.8 and 18.7 mm/h and duration between 1 and 7 hours). The maximum hourly intensity I_{max} was 34 mm/h. As expected, recorded average intensity, I_{av}, decreases with duration, D, thus, on average, long storms are less intense than short storms (Figure 10). About 60% of the events presented an average intensity smaller than 1 mm/h, while about 20% fell within the interval 1-2 mm/h (Figure 11).

An example of the typical slope response during the rainy season is shown in Figure 12, where the hourly values of suction recorded between 20 and 27 January, 2011, are plotted. At the beginning of the week, the shallowest sensor, L2-1, recorded a suction of 13 kPa, while the temperature was around 6°C. Six storms occurred during the considered week, with average intensities between 0.3 and 2.0 mm/h, peak hourly intensities, I_{max}, between 0.8 and 6.2 mm/h, and duration, D, between 6 and 20 hours. No change in suction was observed at any depth after the events I, V and VI, characterized by I_{av} = 0.3-0.7 mm/h, D = 6-12 hours, and a cumulative rainfall height of only 2.1-4.8 mm. Conversely, sensor L2-1 recorded a significant reduction in suction, comprised between 0.7 and 6.0 kPa, after the events II, III and IV, with $0.4 \leq I_{av} \leq 2.0$ mm/h, $17 \leq D \leq 20$ hours, and cumulative rainfall height of 8-38 mm. In particular, Figure 12 shows how storm III caused an acceleration of the suction trends, detected by sensors L2-1 and L2-2, already induced by previous storm II. As shown, the delay in suction decrease with respect to the beginning of the precipitation event, measured by sensor L2-1, was 2-14 hours. The sensor L2-2, placed 40 cm below, recorded suction reductions comprised between 0.8 and 4.7 kPa, thus lower than sensor L2-1, only after the events II and III, with a delay of about 4-16 hours. Finally, suction at the depth of the two deepest tensiometers, L2-3 and L2-4, was affected only by the most intense and long lasting event III, with even smaller reductions (respectively of 3.4 kPa and 3.2 kPa) and a longer delay (6-20 hours).

Figure 13 shows the typical slope response during the warm period (May, 23 - June, 2, 2011, characterized by a mean daily temperature of 21°C and daily temperature excursions up to 12°C). At the beginning of such a period, the suction measured by sensor L2-1 was nearly 16 kPa. In the considered time interval, three 2-4 hours rainfall events occurred, with I_{av} = 3-8 mm/h (corresponding to a cumulative rainfall height of 12.0-17.1 mm) and I_{max} = 4-12 mm/h. None of such events caused any reduction of suction, which instead kept on growing with a nearly constant trend of 0.3 kPa/day at every depth. The small fluctuations in suction shown in Figure 13 are probably related to daily temperature oscillations. In fact, such fluctuations have a period of 24 h,

and all the observed peaks, whose magnitude decreases with depth, occurred at 20:00, about 6 hours after the attainment of the highest daily temperature.

Conversely, during another rain storm occurred in the same season (May, 2 and 3, 2011, when the mean daily temperature was 17°C and the daily temperature excursion about 6°C), a rain storm with similar features, leading to a cumulative rainfall of 11.4 mm, caused a suction drop, from about 8 kPa to about 5 kPa, at z = 0.60 m (L2-1) (Figure 14).

Such a different hydrological response to similar rain storms could be interpreted within a general comprehensive framework accounting for the two main factors affecting the infiltration process: the initial soil moisture conditions (in turn related to weather conditions of the period) and the rain storm features. The first remark is that events with $I_{av} < 1$ mm/h, although typically featured by the highest mean duration (Figure 10), never produce any change in suction. Figure 15 and Figure 16 report the reductions in suction, $\Delta(u_a-u_w)$, recorded by sensor L2-1 at the depth z = 0.60 m during 76 rainfall events with $I_{av} > 1$ mm/h as a function of rainstorm duration and of initial suction, $(u_a-u_w)_0$, measured before each single rainfall event occurred. In particular, Figure 15 summarises the effects of rainfalls with intensities comprised between 1 and 2 mm/h, showing that $\Delta(u_a-u_w)$ is nil for $(u_a-u_w)_0 < 2$ kPa. At the same time, such reduction increases with the growth of initial suction for 2 kPa $< (u_a-u_w)_0 \leq (u_a-u_w)_0^*$, while it decreases with it for $(u_a-u_w)_0 > (u_a-u_w)_0^*$, where $(u_a-u_w)_0^*$ is an observed threshold value that grows with the rainfall duration. A similar result is shown by Figure 16 for more intense rain storms ($3 \leq I_{av} \leq 6$ mm/h), even if field points did not allow to clearly find such suction threshold for $10 < D < 17$ hours: in such case, we can only state that $(u_a-u_w)_0^* > 23$ kPa. In order to explain such a result, it should be noted that the hydrological response of the slope cover depends on the following phenomena, that govern the infiltration process:

i) the capillary potential gradient across the soil surface during rainfall increases with initial suction, $(u_a-u_w)_0$;

ii) the amount of infiltrating water that can be retained by the shallowest soil layer increases with $(u_a-u_w)_0$;

iii) the hydraulic conductivity decreases with $(u_a-u_w)_0$.

Following such considerations, for $(u_a-u_w)_0 < (u_a-u_w)_0^*$, the process seems to be essentially governed by the capillary potential gradient and the capability of the soil to retain water. Conversely, the influence of the reduction of hydraulic conductivity may prevail for $(u_a-u_w)_0 > (u_a-u_w)_0^*$. However, during warm periods, a significant role could be played also by vegetation, that reduces infiltration (Comegna et al. 2013).

4 Conclusions

An automatic field monitoring station has been recently installed at the slope of Cervinara, 50 km North-East of Naples, where a catastrophic rainfall-induced landslide occurred in December 1999. Monitoring consists of simultaneous registration, at high temporal resolution, of rainfall height and of soil suction and volumetric water content at various depths below the ground surface. The data collected during about two years allow to distinguish between the slow seasonal variations of soil suction and water content, which are essentially related to long-term precipitation history (weeks or even months), and the short-term effects of individual rainfall events. The long-term fluctuations affect the initial conditions from which the short-term response of the soil cover begins. In fact, rainfall events generally cause a reduction in suction at shallow depths and a delayed and decreasing reduction at greater depths, but the magnitude of this effect depends either on initial soil conditions or on precipitation features. In warm periods, a significant influence of the temperature has been also noted.

During winter and spring, the average suction measured by the deepest sensors is about 30% smaller than at the shallowest depths. Conversely, during summer and autumn, the highest suction is attained in the deepest layer because of the likely effect of downward local seepage processes. Such a response indicates the importance of the hydraulic conditions at both the top and bottom

boundaries of the soil cover on the hydrological slope response. On the whole, the slope safety factor estimated during the monitoring period should fluctuate between 1.1 and 1.8.

The short-term reduction in suction measured by the shallowest sensors, caused by a given storm, tends to increase of about 80% if the initial suction doubles: such a result has been observed up to a suction threshold value, beyond which the response is opposite. Therefore, the effects of rainfall on soil moisture variations are strongly influenced by the initial conditions of the soil. Such observations explain the limited reliability of the empirical threshold models usually adopted for the assessment of landslide triggering, which are exclusively based on the characteristics of precipitations, typically intensity and duration, without taking into account the major role played by the hydraulic properties and the initial state of the soil.

The initial conditions of the soil, instead, should be considered as the preconditions for the soil cover to be significantly affected by single rainfall events, i.e. the long-term causes predisposing the short-term triggering of landslides.

5 Acknowledgements

The research has been developed with the support and partial funding by the European Project "*SafeLand - Living with landslide risk in Europe: assessment, effects of global change, and risk management strategies*", funded by the 7th Framework Programme for research and technological development (FP7) of the European Commission.

The Civil Protection Department is gratefully acknowledged for providing rainfall and temperature data.

6 References

Brooks, R.H. and Corey, A.T. 1964. Hydraulic properties of porous media. Hydrology Paper No.3, Colorado State University, Fort Collins, Colorado.

Cascini, L. and Sorbino, G. 2004. The contribution of soil suction measurements to the analysis of flowslides triggering. *In* Proceedings of the International Workshop on "Occurrence and mechanisms of flow-like landslides in natural slopes and earthfills", Sorrento, Italy, 14–16 May 2003, Pàtron Editore, Bologna, pp 77–85.

Cascini, L., Sorbino, G., Cuomo, S. and Ferlisi, S. 2014. Seasonal effects of rainfall on the shallow pyroclastic deposits of the Campania region (southern Italy). Landslides, **11**:779-792.

Chae, B.-G., and Seo, Y.S. 2012. An alternative method for landslide early warning based on gradient of volumetric water content in unsaturated soil. Landslides and Engineered Slopes: Protecting Society through Improved Understanding. *In* Proceedings of the XI International Symposium on Landslides, Banff, Alberta, Canada, 2 – 8 June 2012, Vol. 2, pp. 1457-1463.

Collins, B.D., Stock, J.D., Foster, K.A., Whitman, M.P.W. and Knepprath, N.E. 2012. Monitoring the subsurface hydrologic response for precipitation-induced shallow landsliding in the San Francisco Bay area, California, USA. Landslides and Engineered Slopes: Protecting Society through Improved Understanding. *In* Proceedings of the XI International Symposium on Landslides, Banff, Alberta, Canada, 2 – 8 June 2012, Vol. 2, pp. 1249-1255.

Comegna, L., Damiano, E., Greco, R., Guida, A., Olivares, L. and Picarelli, L. 2013. Effects of the vegetation on the hydrological behavior of a loose pyroclastic deposit. Procedia Environmental Science, **19**:922-931. doi: 10.1016/j.proenv.2013.06.102.

Comegna, L., Damiano, E., Greco, R., Guida, A., Olivares, L., and Picarelli L. 2016a. Investigation on the hydraulic hysteresis of a pyroclastic deposit. *In* Proceedings of the International Workshop on Volcanic Rocks and Soils, Isle of Ischia, Italy, 24-25 September 2015, Taylor & Francis Group, London, pp 313-317.

Comegna, L., Guida, A., Damiano, E., Olivares, L., Greco, R. and Picarelli, L. 2011. Monitoraggio di un pendio naturale in depositi piroclastici sciolti. *In* Proceedings of the XXIV Convegno Nazionale di Geotecnica, Naples, 22 – 24 June 2011. Edizioni Associazione Geotecnica Italiana, Roma, Vol. 2, pp. 681-686.

Comegna, L., Rianna, G., Lee, S-G., and Picarelli, L. 2016b. Influence of the wetting path on the mechanical response of shallow unsaturated sloping covers. Computers and Geotechnique, **73**:164-169.

Cui, Y-J, Ta, A.N., Hemmati, S., Tang, A.M., and Gatmiri, B. 2012. Experimental and numerical investigation of soil-atmosphere interaction. Engineering Geology, **165**:20-28.

Damiano, E., Olivares, L., and Picarelli, L. 2012. Steep-slope monitoring in unsaturated pyroclastic soils. Engineering Geology, **137-138**:1-12. doi: 10.1016/j.enggeo.2012.03.002.

Evangelista, A., Nicotera, M.V., Papa, R., and Urciuoli, G. 2008. Field investigation on triggering mechanisms of fast landslides in unsaturated pyroclastic soils. *In* Proceedings of the 1st European Conference on Unsaturated Soil, Durham, United Kingdom, 2–4 July 2008. Taylor and Francis Group plc, London, pp 909–915.

Fiorillo, F., Guadagno, F.M., Equino, S., and De Blasio, A. 2001. The December 1999 Cervinara landslides: further debris flows in the pyroclastic deposits of Campania (southern It-aly). Bull. Eng. Geol. Env., **60**(3): 171-184.

Fredlund, D.G. and Rahardjo, H. 1993. Soil mechanics for unsaturated soils. Wiley, New York.

Fusco, F., De Vita, P., Napolitano, E., Allocca, V., and Manna, F. 2013. Monitoring the soil suction regime of landslide-prone ash-fall pyroclastic deposits covering slopes in the Sarno area (Campania - southern Italy). Rend. Online Soc. Geol. It., **24**:146-148.

Greco, R., Comegna, L., Damiano, E., Guida, A., Olivares, L., and Picarelli, L. 2013. Hydrological modelling of a slope covered with shallow pyroclastic deposits from field monitoring data. Hydrology and Earth System Sciences, **17**:4001-4013. doi: 10.5194/hess-17-4001-2013.

Greco, R., Comegna, L., Damiano, E., Guida, A., Olivares, L., and Picarelli, L. 2014. Conceptual hydrological modeling of the soil-bedrock interface at the bottom of the pyroclastic cover of Cervinara (Italy). Procedia Earth and Planetary Science, **9**:122–131. doi: 10.1016/j.proeps.2014.06.007.

Guadagno, F.M., Revellino, P. and Grelle, G. 2011. The 1998 Sarno landslides: conflicting interpretations of a natural event. *In* Proceedings of the 5th International Conference on Debris-Flow Hazards Mitigation: Mechanics, Prediction and Assessment. Italian Journal of Engineering Geology and Environment. Casa Editrice Università La Sapienza, www.ijege.uniroma1.it. doi: 10.4408/IJEGE.2011-03.B-009.

Guida, A., Comegna, L., Damiano, E., Greco, R., Olivares, L., and Picarelli, L. 2012. Soil characterization from monitoring over steep slopes in layered granular volcanic deposits. *In* Proceedings of The second Italian Workshop on Landslides, Naples, 28 – 30 September 2011. *Edited by* L. Picarelli, R. Greco and G. Urciuoli, Cooperativa Universitaria Editrice Studi, Fisciano, pp. 147-153.

Harris, S.J., Orense, R.P. and Itoh, K. 2012. Back analyses of rainfall-induced slope failure in Northland Allochthon formation. Landslides, **9**(3): 349-356. doi: 10.1007/s10346-011-0309-1.

Hawke, R., and McConchie, J. 2011. In situ measurement of soil moisture and pore-water pressures in an 'incipient' landslide: Lake Tutira, New Zealand. Journal of Environmental Management, **92**(2):266–274.

Hubbert, K.R., Beyers, J.L., and Graham, R.C. 2001. Roles of weathered bedrock and soil in seasonal water relations of *Pinus jeffreyi* and *Arctostaphylos patula*, Canadian Journal of Forest Research, **31**:1947–1957.

Li, A.G., Yue, Z.Q., Tham, L.G., Lee, C.F., and Law, K.T. 2005. Field-monitored variations of soil moisture and matric suction in a saprolite slope. Canadian Geotechnical Journal, **42**(1): 13–26.

Mancarella, D., Doglioni, A., and Simeone, V. 2012. On capillary barrier effects and debris slide triggering in unsaturated soil covers. Engineering Geology, **147-148**:14-27.

McCole, A.A., and Stern, L.A. 2007. Seasonal water use patterns of *Juniperus ashei* on the Edwards Plateau, Texas, based on stable isotopes in water. Journal of Hydrology, **342**:238-248.

Napolitano, E., De Vita, P., Fusco, F., Allocca, V., and Manna, F. 2015. Long-Term Hydrological Modelling of Pyroclastic Soil Mantled Slopes for Assessing Rainfall Thresholds Triggering Debris Flows: The Case of the Sarno Mountains (Campania—Southern Italy). Engineering Geology for Society and Territory. *Edited by* G. Lollino et al., Springer International Publishing Switzerland, Vol. 2. doi: 10.1007/978-3-319-09057-3_278.

Nie, Y.P., Chen, H.S., Wang, K.L. and Yang, J. 2012. Water source utilization by woody plants growing on dolomite outcrops and nearby soils during dry seasons in karst region of Southwest China. Journal of Hydrology, **420**:264–274.

Olivares, L., Andreozzi, L., Damiano, E., Avolio, B., and Picarelli, L. 2003. Hydrologic response of a steep slope in unsaturated pyroclastic soils. *In* Proceedings of the Int. Conf. on Fast Slope Movements — Prediction and Prevention for Risk Mitigation, Naples, 11–13 May 2003. *Edited by* L. Picarelli, Pàtron Editore, Bologna, Vol. 1, pp. 391–398.

Olivares, L., Damiano, E., Greco, R., Zeni, L., Picarelli, L., Minardo, A., Guida, A., and Bernini, R. 2009. An instrumented flume to investigate the mechanics of rainfall-induced landslides in unsaturated granular soils. Geotech Test J, **32**(2):108-118.

Olivares, L., and Picarelli, L. 2003. Shallow flowslides triggered by intense rainfalls on natural slopes covered by loose unsaturated pyroclastic soils. Geotechnique, **53**(2):283–288.

Olivares, L., and Tommasi, P. 2008. The role of suction and its changes on stability of steep slopes in unsaturated granular soils. *In* Proceedings of the 10th International Symposium on Landslides and Engineered Slopes, Xi'an (China), 30 June – 4 July 2008. *Edited by* Z. Chen , J. Zhang , Z. Li , F. Wu and K. Ho, CRC Press, pp. 203-215.

Picarelli L., Evangelista A., Rolandi G., Paone A., Nicotera M.V., Olivares L., Scotto di Santolo, A., Lampitiello, S., and Rolandi, M. 2006. Mechanical properties of pyroclastic soils in

Campania Region. *In* Proceedings of the 2nd Int. Work. on Characterisation and Engineering Properties of Natural Soils, Singapore, Vol. 3, pp. 2331–2383.

Pirone, M., Papa, R., and Nicotera, M.V. 2010. Test site experience on mechanisms triggering mudflows in unsaturated pyroclastic soils in southern Italy. *In* Proceedings of the 5th International Conference on Unsaturated Soils — Unsaturated Soils, Barcelona, Spain, 6–8 September 2010. CRC Press/Balkema, Leiden, Vol. 2, pp 1273–1278.

Pirone, M., Papa, R., Nicotera, M.V., and Urciuoli, G. 2014. Evaluation of the hydraulic hysteresis of unsaturated pyroclastic soils by in situ measurements. Procedia Earth and Planetary Science, **9**:163-170.

Querejeta, J.I., Estrada-Medina, H., Allen, M.F., Jimenez-Osornio, J.J., and Ruenes, R. 2006. Utilization of bedrock water by Brosimum alicastrum trees growing on shallow soil atop limestone in a dry tropical climate. Plant Soil, **287**:187–197.

Querejeta, J.I., Estrada-Medina, H., Allen, M.F., and Jiménez-Osornio, J.J. 2007. Water source partitioning among trees growing on shallow karst soils in a seasonally dry tropical climate. Oecologia, **152**:26-36.

Smith, J.B., Godt, J.W., Baum, R. L., Coe, J.A., Burns, W.J., Lu, N., Morse, M. M., SenerKaya, B., and Kaya, M. 2014. Hydrologic monitoring of a landslide-prone hillslope in the Elliott State Forest, Southern Coast Range, Oregon, 2009–2012. U.S. Geological Survey Open-File Report, 2013–1283, U.S. Geological Survey, Reston, VA.

Topp, G.C., Davis, J.L., and Annan, A.P. 1980. Electromagnetic determination of soil water content: measurement in coaxial transmission lines. Water Resour. Res., **16**:574-582.

Trandafir, A.C., Sidle, R.C., Gomi, T., and Kamai, T. 2008. Monitored and simulated variations in matric suction during rainfall in a residual soil slope. Environ Geol, **55**:951-961

Tsaparas, I., Rahardjo, H., Toll, D.G., and Leong, E.-C. 2003. Infiltration characteristics of two instrumented residual soil slopes. Canadian Geotechnical Journal, **40**:1012-1032.

van Genuchten, M.Th. 1980. A closed-form equation for predicting the hydraulic conductivity of unsaturated soil. Soil Science Society of America Journal, **44**:615–628.

Zhan, T.L.T., Ng, C.W.W. and Fredlund, D.G. 2007. Field study of rainfall infiltration into a grassed unsaturated expansive soil slope. Canadian Geotechnical Journal, **44**:392-408.

7 Figure captions

Figure 1. Plan view of the instrumented site and of the landslide occurred in Cervinara on December, 1999 (modified from Damiano et al. 2012).

Figure 2. Grain size distribution of the various layers (modified from Damiano et al. 2012).

Figure 3. Stratigraphy recognized by pits executed near nest 1 (a) and nest 2 (b) of the automatic monitoring station: i) humified volcanic ashes (Top Soil); ii) coarse pumices (Layer B); iii) volcanic ashes (Layer B); iv) altered ashes (Layer D); v) fractured calcareous bedrock.

Figure 4. Hourly values of rainfall h, temperature T, suction u_a-u_w, and volumetric water content θ measured at nest 1 from December, 2009 to August, 2010.

Figure 5. Hourly values of rainfall h, temperature T, suction u_a-u_w and volumetric water content θ measured at nest 2 from January, 2011 to December, 2011.

Figure 6. Monthly rainfall together with mean daily temperature and mean suction, measured at nest 2 from January, 2011 to January, 2012.

Figure 7. Hourly rainfall h and suction u_a-u_w measured at nest 1 (sensor L1-2) and nest 2 (sensor L2-2) from January to July, 2011.

Figure 8. Measurements from January to July, 2011: hourly rainfall h and mean daily temperature T (a); vertical hydraulic gradient calculated at nest 2 (b); suction profiles measured at nest 2 on January, 12 (c), March, 17 (d) and July, 27 (e).

Figure 9. Water retention curves obtained from in situ monitoring at different depths.

Figure 10. Features of the rainfall events occurred from 2002 to 2011 in Cervinara site: average intensity, I_{av}, and duration, D.

Figure 11. Frequency distribution of average intensity, I_{av}, of rainfall events, observed from 2002 to 2011 in Cervinara.

Figure 12. Hourly suction response to six consecutive storms during winter (January, 2011).

Figure 13. Hourly suction response to three rainfall events during the warm season (May, 2011).

.

Figure 14. Hourly suction response to a rainfall event during the warm season (May, 2011).

Figure 15. Rain storms occurred in 2011 with average intensity I_{av} = 1-2 mm/h: reduction in suction $\Delta(u_a-u_w)$ as a function of the initial value $(u_a-u_w)_0$, recorded at nest 2 by sensor L2-1 (z = 0.60 m).

Figure 16. Rain storms occurred in 2011 with average intensity I_{av} = 3-6 mm/h: reduction in suction $\Delta(u_a-u_w)$ as a function of the initial value $(u_a-u_w)_0$, recorded at nest 2 by sensor L2-1 (z = 0.60 m).

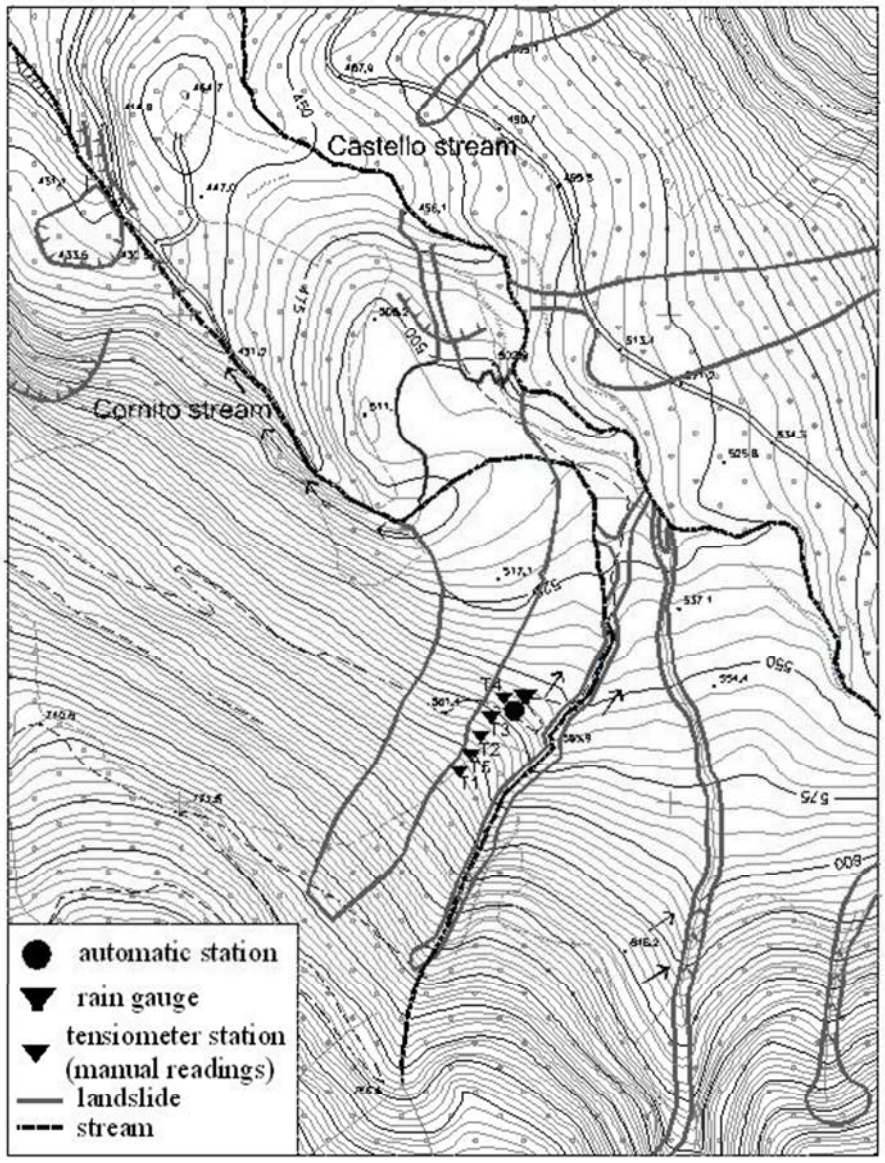

Figure 1. Plan view of the instrumented site and of the landslide occurred in Cervinara on December, 1999 (modified from Damiano et al. 2012).
96x123mm (150 x 150 DPI)

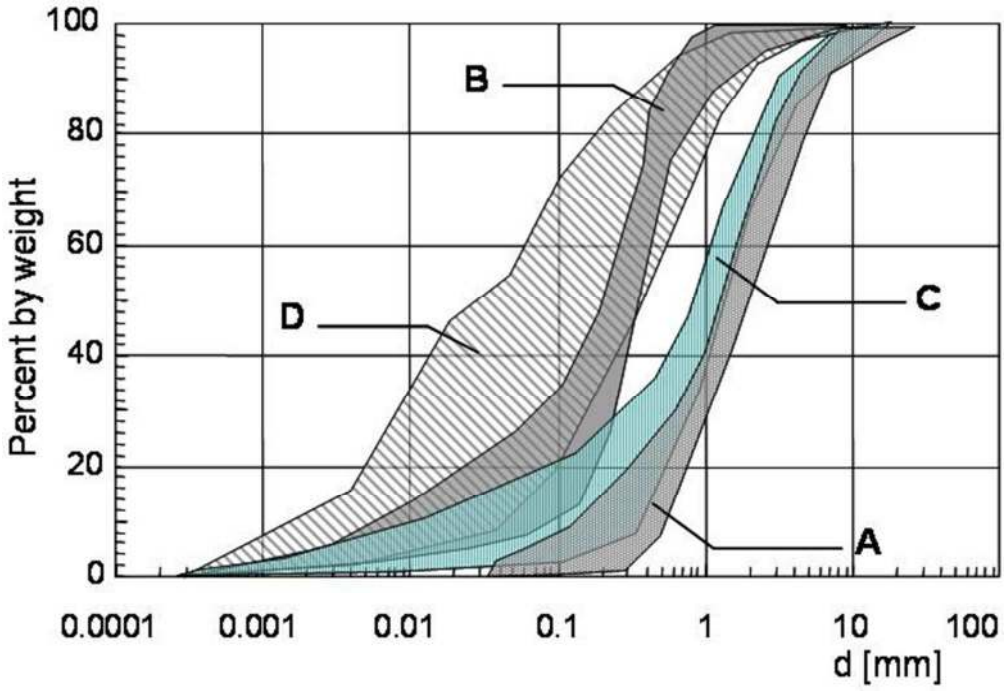

Figure 2. Grain size distribution of the various layers (modified from Damiano et al. 2012).
109x75mm (150 x 150 DPI)

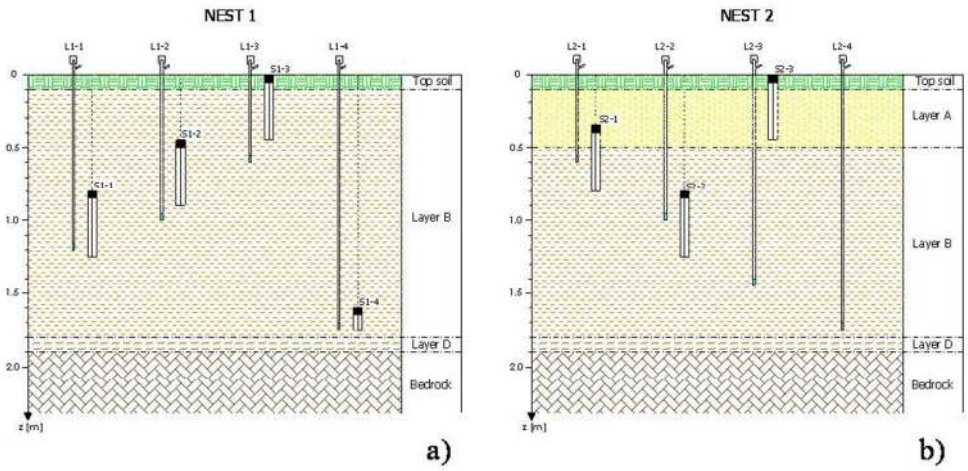

Figure 3. Stratigraphy recognized by pits executed near nest 1 (a) and nest 2 (b) of the automatic monitoring station: i) humified volcanic ashes (Top Soil); ii) coarse pumices (Layer B); iii) volcanic ashes (Layer B); iv) altered ashes (Layer D); v) fractured calcareous bedrock.
175x84mm (150 x 150 DPI)

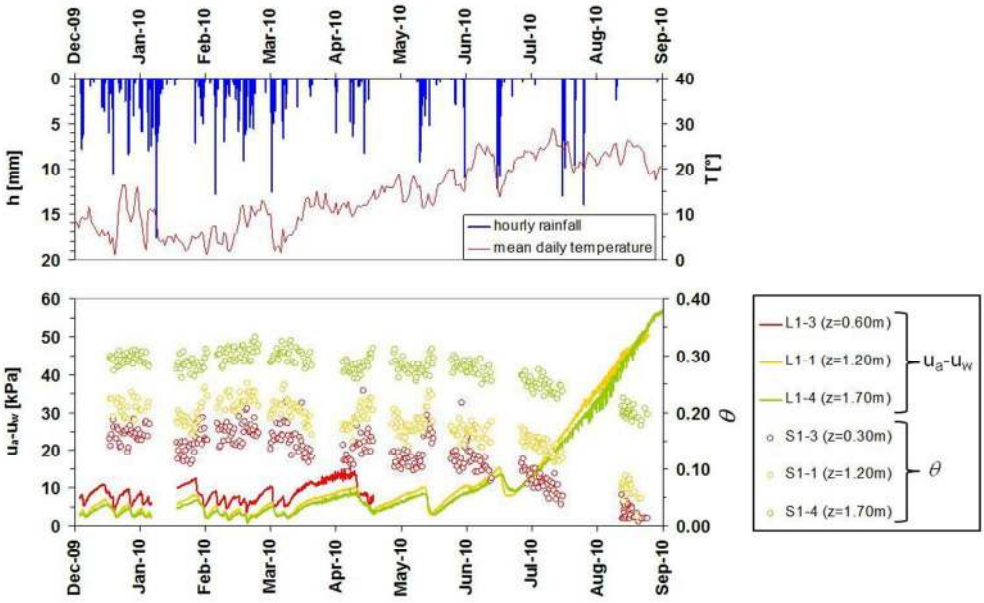

Figure 4. Hourly values of rainfall *h*, temperature *T*, suction u_a-u_w, and volumetric water content θ measured at nest 1 from December, 2009 to August, 2010.
192x126mm (150 x 150 DPI)

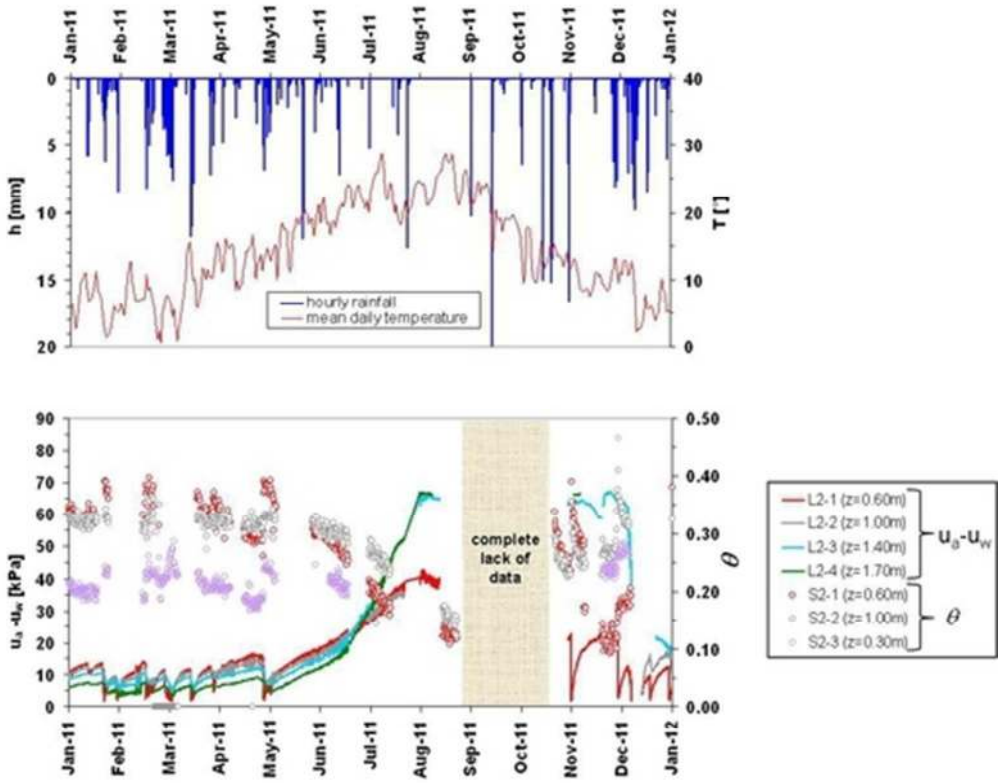

Figure 5. Hourly values of rainfall *h*, temperature *T*, suction u_a-u_w *and volumetric water content θ measured at nest 2 from January, 2011 to December, 2011.*
180x153mm (72 x 72 DPI)

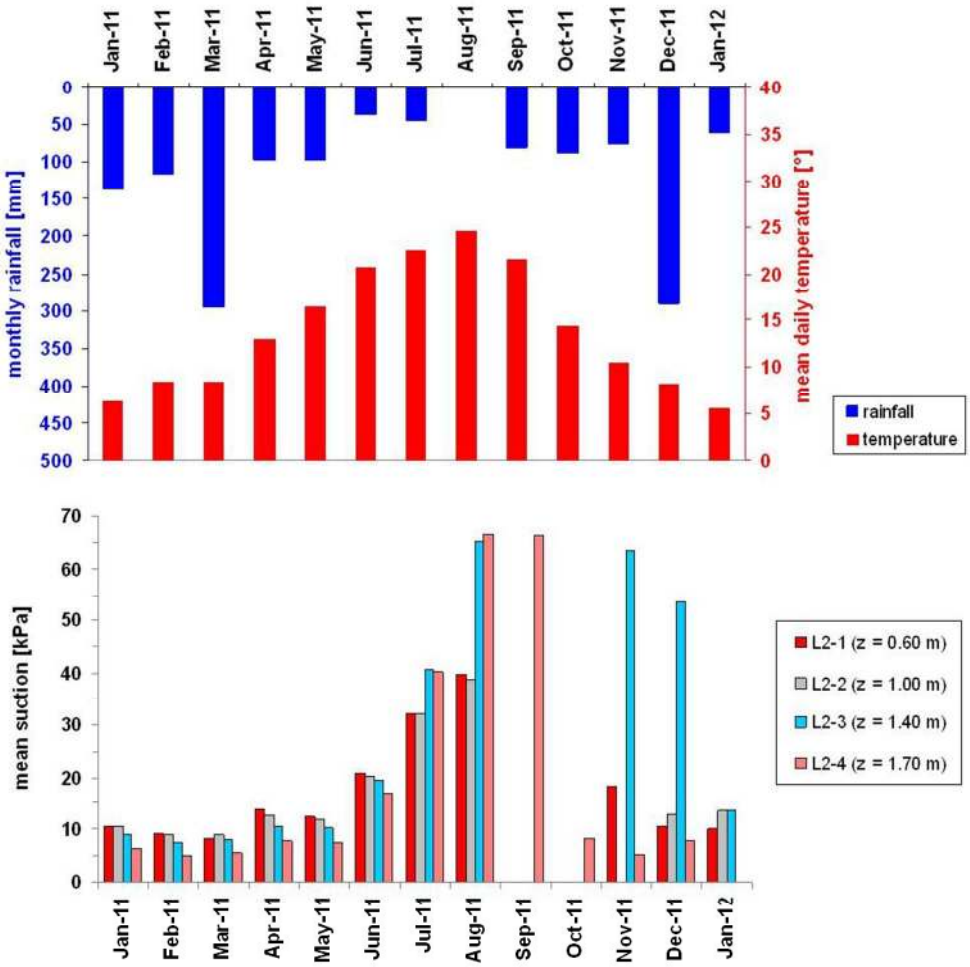

Figure 6. Monthly rainfall together with mean daily temperature and mean suction, measured at nest 2 from January, 2011 to January, 2012.
169x173mm (150 x 150 DPI)

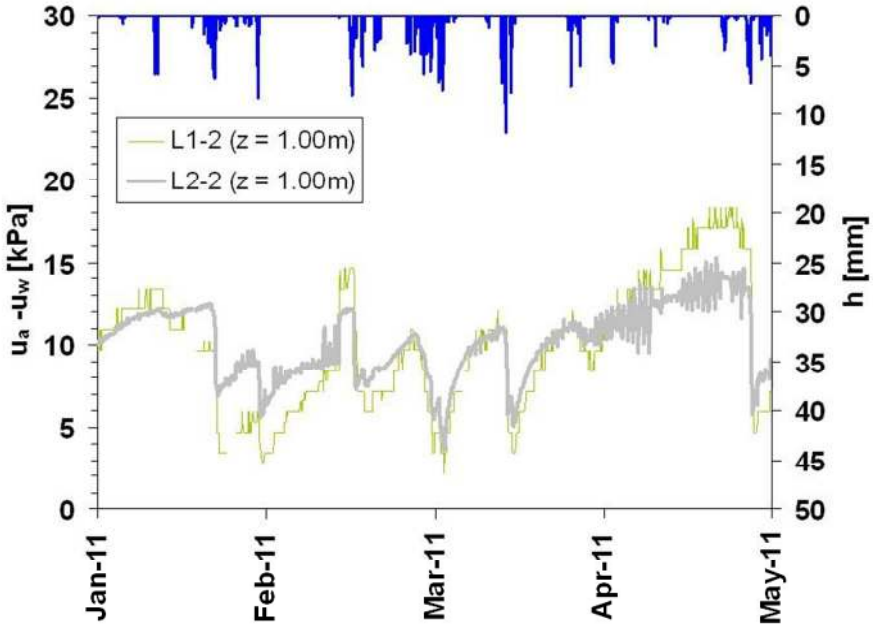

Figure 7. Hourly rainfall *h* and suction u_a-u_w measured at nest 1 (sensor L1-2) and nest 2 (sensor L2-2) from January to July, 2011.
169x112mm (150 x 150 DPI)

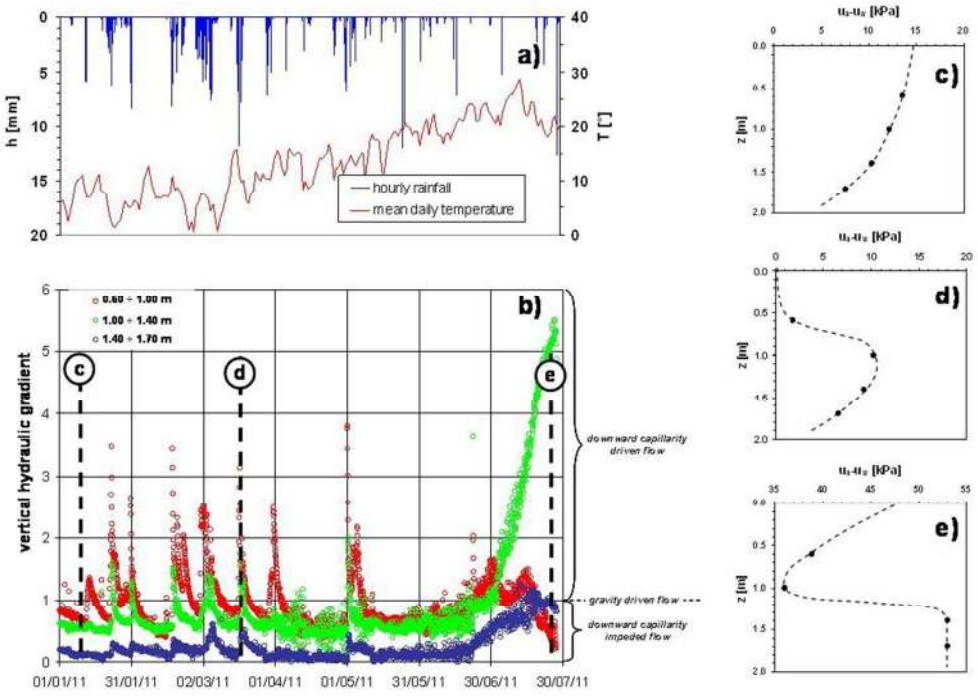

Figure 8. Measurements from January to July, 2011: hourly rainfall *h* and mean daily temperature *T* (a); vertical hydraulic gradient calculated at nest 2 (b); suction profiles measured at nest 2 on January, 12 (c), March, 17 (d) and July, 27 (e).
169x122mm (150 x 150 DPI)

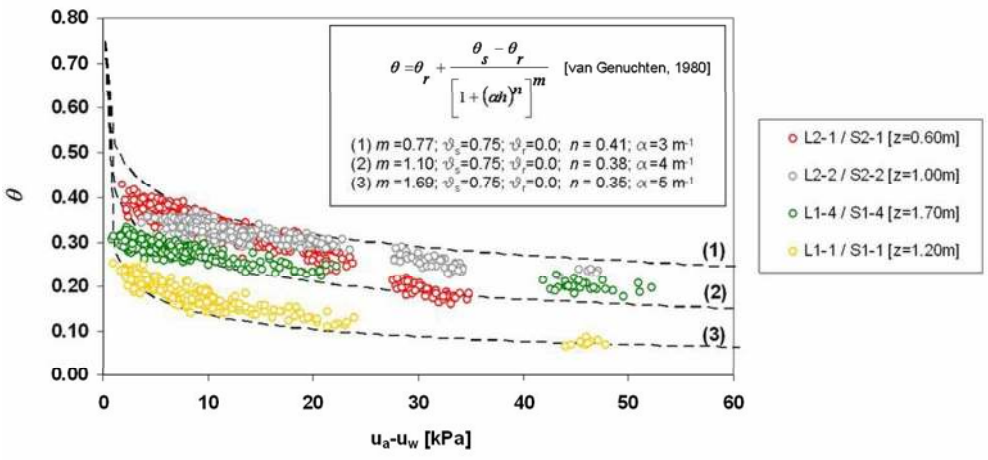

Figure 9. Water retention curves obtained from in situ monitoring at different depths.
169x77mm (150 x 150 DPI)

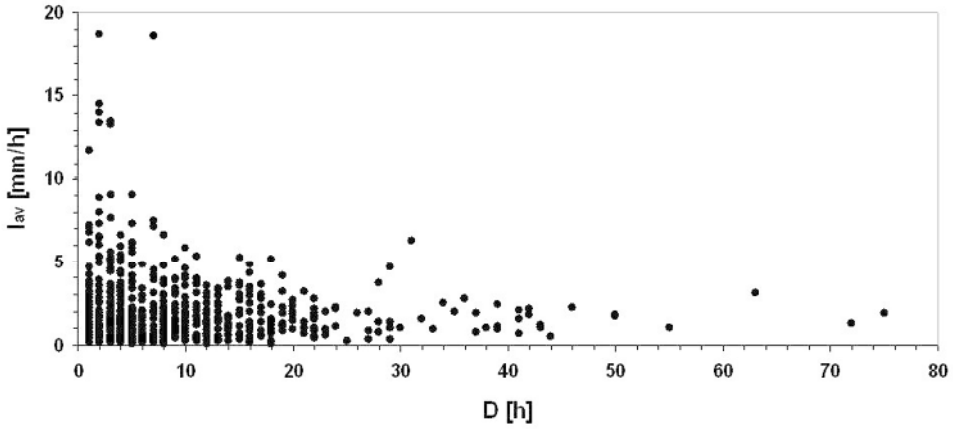

Figure 10. Features of the rainfall events occurred from 2002 to 2011 in Cervinara site: average intensity, I_{av}, and duration, D.
169x81mm (150 x 150 DPI)

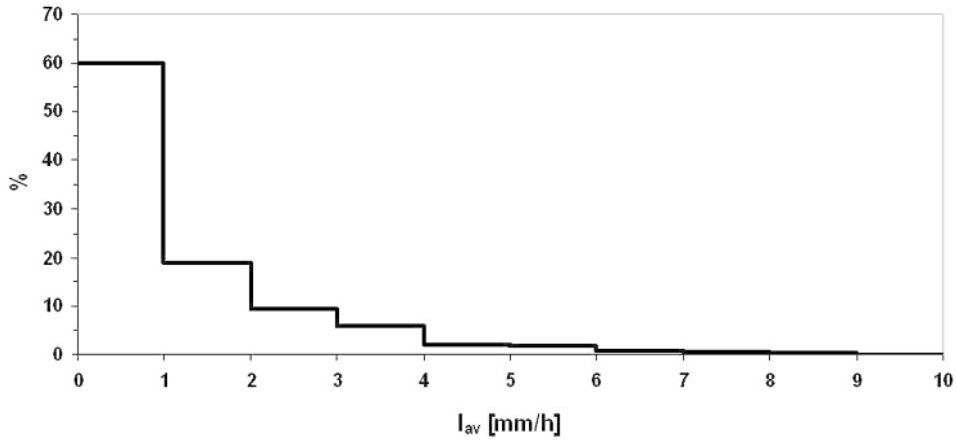

Figure 11. Frequency distribution of average intensity, I_{av}, of rainfall events, observed from 2002 to 2011 in Cervinara.
169x83mm (150 x 150 DPI)

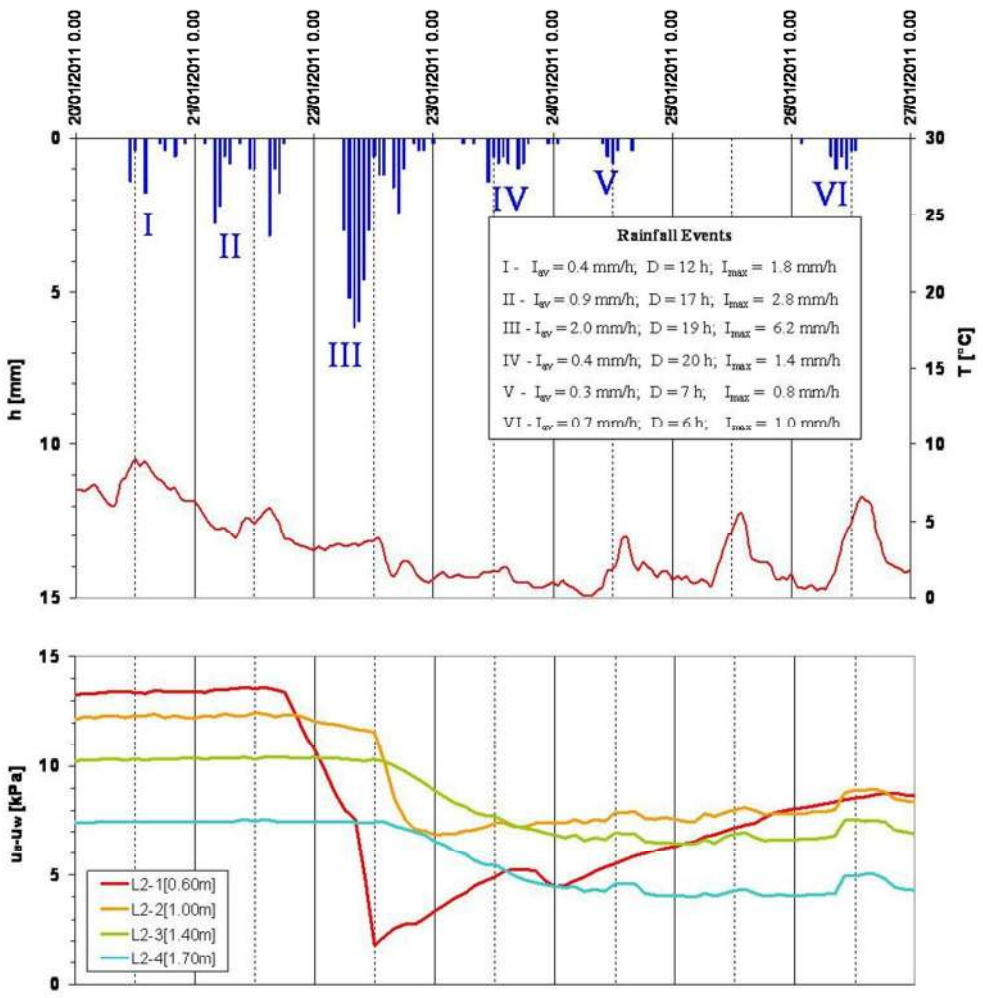

Figure 12. Hourly suction response to six consecutive storms during winter (January, 2011).
169x179mm (150 x 150 DPI)

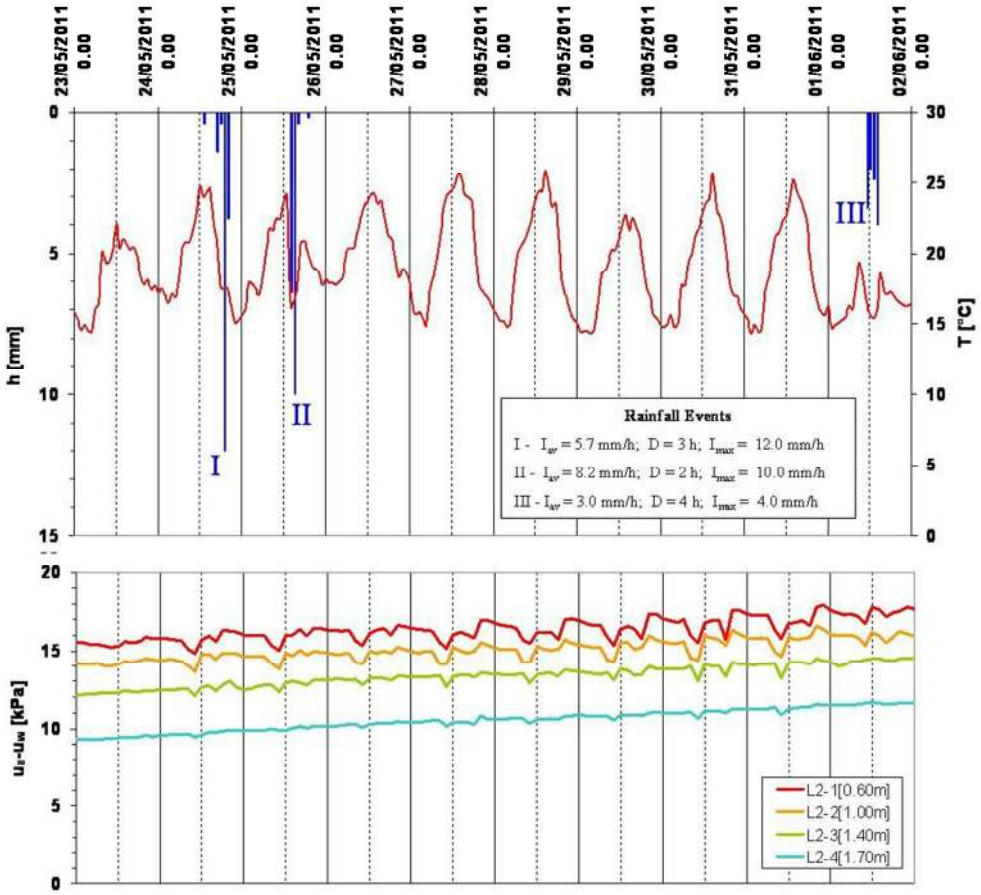

Figure 13. Hourly suction response to three rainfall events during the warm season (May, 2011).
169x165mm (150 x 150 DPI)

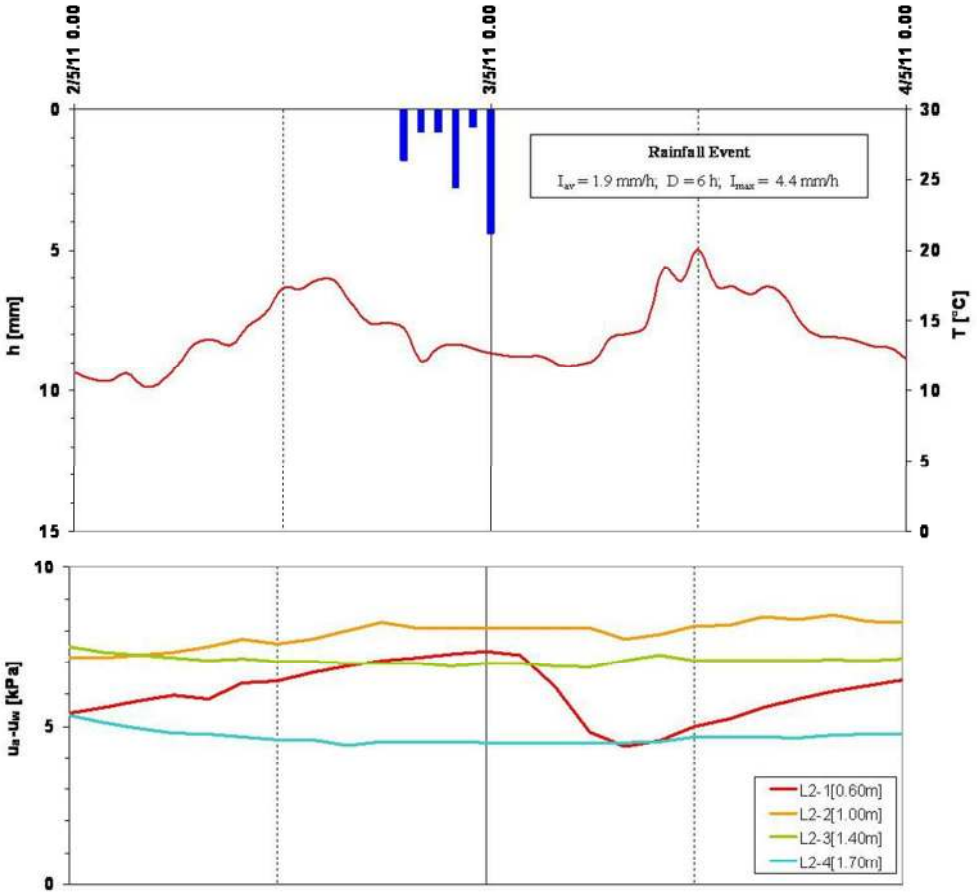

Figure 14. Hourly suction response to a rainfall event during the warm season (May, 2011).
171x168mm (150 x 150 DPI)

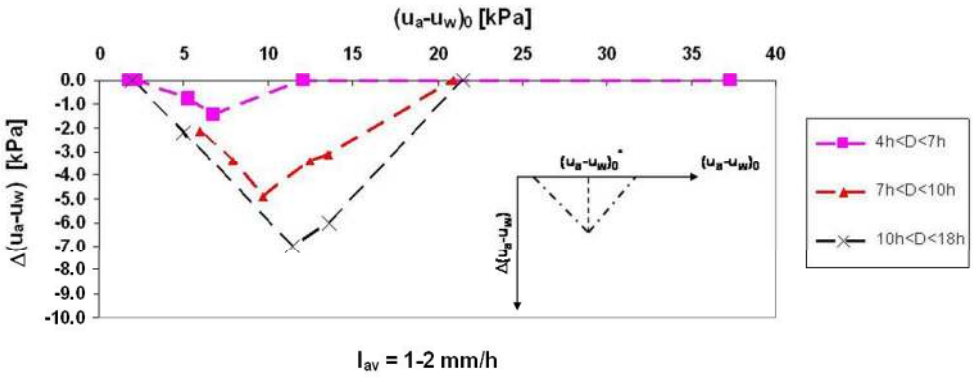

Figure 15. Rain storms occurred in 2011 with average intensity I_{av} = 1-2 mm/h: reduction in suction $\Delta(u_a-u_w)$ as a function of the initial value $(u_a-u_w)_0$, recorded at nest 2 by sensor L2-1 (z = 0.60 m).
175x77mm (150 x 150 DPI)

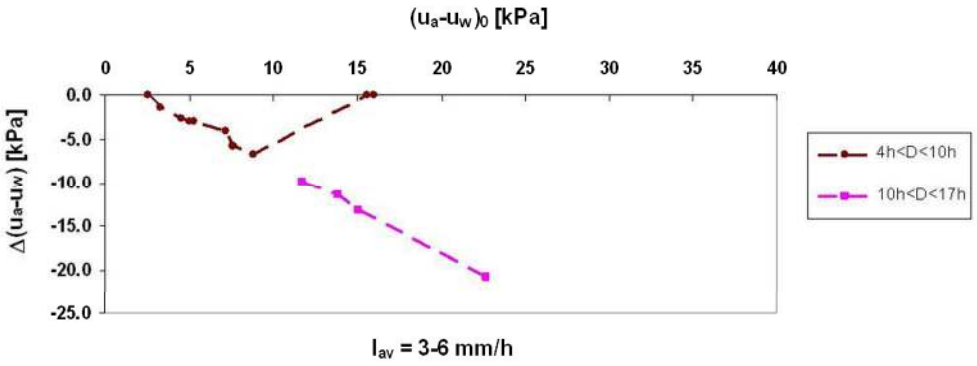

Figure 16. Rain storms occurred in 2011 with average intensity I_{av} = 3-6 mm/h: reduction in suction $\Delta(u_a-u_w)$ as a function of the initial value $(u_a-u_w)_0$, recorded at nest 2 by sensor L2-1 (z = 0.60 m).
175x74mm (150 x 150 DPI)

Table 1. Soil properties obtained in laboratory: specific unit weight, γ_s, unit weight, γ, porosity, n, effective cohesion, c', effective friction angle, φ', hydraulic conductivity, k, apparent cohesion, c, measured at different effective mean stress p' (for saturated samples) or mean suction u_a-u_w (for unsaturated samples).

				saturated samples			unsaturated samples	
Layer	γ_s[kN/m^3]	γ[kN/m^3]	n [%]	k [m/s]	c' [kPa]	φ' [°]	k [m/s]	c [kPa]
				(p' = 20 - 100 kPa)	(p' = 20 - 150 kPa)		(u_a-u_w = 0 - 80 kPa)	(u_a-u_w = 2 - 80 kPa)
A	25	13	52	3E-06 - 7E-06	-	-	-	-
B	26	14	70	1E-06 - 6E-06	0	38	1E-08 - 1E-06	1.5 - 10
C	26	14	50	3E-07 - 8E-07	-	-	-	-
D	26	16	60	8E-07 - 1E-06	11	31	-	-

Table 2. Minimum and maximum suction measured from December, 2009 to August, 2010.

	L1-3 [0.60m]		L1-1 [1.20m]		L1-4 [1.70m]	
	MIN [kPa]	MAX [kPa]	MIN [kPa]	MAX [kPa]	MIN [kPa]	MAX [kPa]
December, 2009	3.8	10.9	2.2	6.8	2.1	5.5
January, 2010	4.4	12.3	2.1	8.1	2.1	6.7
February, 2010	2.4	9.2	0.9	5.1	0.7	4.0
March, 2010	5.0	12.8	2.1	8.1	1.9	7.0
April, 2010	4.8	15.6	3.5	10.0	3.1	9.8
May, 2010	-	-	3.1	10.1	2.8	8.5
June, 2010	-	-	7.6	15.2	7.4	13.5
July, 2010	-	-	10.4	33.2	10.1	30.0
August, 2010	-	-	32.1	50.8	27.2	55.0

Table 3. Minimum and maximum suction measured from January, 2011 to December, 2011.

	L2-1 [0.60m]		L1-2 [1.00m]		L2-2 [1.00m]		L2-3 [1.40m]		L2-4 [1.70m]	
	MIN [kPa]	MAX [kPa]	MIN [kPa]	MAX [kPa]	MIN [kPa]	MAX [kPa]	MIN [kPa]	MAX [kPa]	MIN [kPa]	MAX [kPa]
January, 2011	1.8	13.6	2.8	13.4	5.6	12.5	5.7	10.4	3.3	7.6
February, 2011	2.4	14.0	3.4	14.6	6.3	12.1	5.7	10.4	3.2	7.7
March, 2011	1.8	12.5	2.2	12.1	3.6	11.5	4.2	9.6	3.0	6.7
April, 2011	2.0	16.7	8.4	18.3	9.6	15.3	8.7	12.2	6.0	9.1
May, 2011	2.1	17.9	4.6	22.0	5.8	16.6	6.8	14.5	4.4	11.6
June, 2011	16.3	27.7	20.8	43.2	15.0	29.0	13.9	28.8	11.5	27.2
July, 2011	25.0	39.1	40.7	61.8	26.4	36.2	28.0	53.0	27.1	53.0
August, 2011	37.0	42.9	61.2	68.0	-	-	63.0	66.3	65.8	67.1
September, 2011	-	-	-	-	-	-	-	-	-	-
October, 2011	-	-	-	-	-	-	-	-	-	-
November, 2011	1.9	23.1	73.0	81.7	42.7	48.6	58.9	67.2	65.9	66.7
December, 2011	2.1	10.4	3.4	11.5	7.8	16.3	20.6	21.9	-	-